

Developing an innovating optimization framework for enhancing the long-term energy system resilience against climate change disruptive events



Somayeh Ahmadi^{a,b}, Amir Hossein Fakih Khorasani^c, Ali Vakili^{c,*}, Yadollah Saboohi^b, Georgios Tsatsaronis^a

^a Institute for Energy Engineering, Technische Universität Berlin, 10587, Berlin, Germany

^b Energy Engineering Department, Sharif University of Technology, P.O. Box 11365-9567, Tehran, Iran

^c Research Institute for Energy Management and Planning, Tehran University, P.O. Box 1417466191, Tehran, Iran

ARTICLE INFO

Keywords:

Energy system resilience
Climate change
Long-term optimization framework
Critical infrastructure

ABSTRACT

The energy system is one of the major sub-sectors of the economy in every society in which both supply with high reliability and compatibility of the energy sector with the environment is a necessity in the process of economic reconstruction and sustainable development. The energy system has been more susceptible to various disruptive events in recent years. Thus, designing a resilient energy system capable of resisting and recovering rapidly from high-impact low-probability (HILP) disruptive events is essential. This paper focuses on developing a two-stage long-term optimization framework for evaluating the energy system resilience as a crucial Critical Infrastructure (CI) system against HILP caused by climate change. The results show the share of electricity generation shift from coal and hydropower to PV in different scenarios based on the maximization of energy system resiliency. The faster occurring this shift, the greater vulnerability of the system. Furthermore, the sensitivity analysis of the optimum solution shows that the vulnerability of energy systems against HILP events depends on planner flexibility.

1. Introduction

Nowadays, increased disruption risks on the one hand, and a high degree of interconnectedness between energy systems infrastructure and other critical infrastructure systems, on the other hand, require analysis methods to evaluate the impact of disruptive events on energy systems that can strongly affect both economic and social activities depending on a reliable and efficient supply of energy [1–4]. As a Critical Infrastructure (CI), energy is essential for forecasting both governance and providing goods and services. Thus, the high-level security and reliability of this infrastructure are fundamental [5]. Indeed, energy systems should be highly resilient to the effects of internal and external variations, changes, disturbances, disruptions, and surprises. Climate change is one of the most problematic issues causing several disruptions in various social and economic systems [6]. The energy system is one of the major sub-sectors of the economy in every society in which both supply with high reliability and compatibility of the energy sector with the environment is a necessity in the process of economic reconstruction and sustainable development.

Energy systems have a dual relationship to climate change; hence, the energy sector drives climate change due to greenhouse gas emissions, and the operation of energy systems is seriously affected by the climate change impacts. Also, considering the complex relationship between socio-economic and energy systems, evaluating the risks, threats, and disruptions of the energy supply and demand system due to climate change are among the most critical energy planning and policymaking [7]. Climate change can negatively impact people's satisfaction through the lack of satisfaction of the energy demand or through rising prices for goods and services, which might be directly dependent on rising energy prices, and through disruptions to water supply and food production. Therefore, considering the uncertainties, disruptions, and hazards of the external environment through energy systems, resilience is one of the ways to deal with climate change disruptions [8] because this will consider the optimal path for sustainable development of the energy sector and will minimize the risks of climate change uncertainties in the decision-making process. Resilience is a strategy for risk management; its goal is to minimize vulnerability, improve flexibility, adapt to the surrounding environment, and increase the system's

* Corresponding author.

E-mail address: vakiliali55@gmail.com (A. Vakili).

tolerance in the face of threats and system disturbances.

Energy security is a multifaceted term divided into resilience and system reliability when facing various disruptive events and shocks to the system. Differences in these two basic pillars of energy security are described by Pantel and Mancarla and other researchers [9–11], where the authors argue that system reliability deals with low-intensity and high-probability (LIHP) events. In contrast, system resilience deals with high-intensity and low-probability (HILP) disruptive events. Hence, energy system resilience deals with the context of high-impact low-probability (HILP) disruptive events [11–14] as HILP resulted from climate change. Climate change and increased weather variability have significantly impacted CI and economic properties [15,16]. For example, Superstorm Sandy was an extreme weather event exacerbated by climate change and caused about \$60 billion in damages because of power outages and fuel shortages [17]. Hines et al. calculated the size of North American electricity blackout using the observed statistical trends for 100 years according to these disasters, which was about 186,000 MW [18]. Also, it is expected to increase the number and severity of disruptive events resulting in global warming and climate change in the future.

Therefore, considering the energy system resilience and related models, framework and tools for the protection of energy system and support of decision-makers are necessary. Critical infrastructure resilience models are addressed conceptually in a wide range of studies, where optimization approaches are typically used to evaluate the resilience of systems. Various studies have been conducted in the context of energy resilience into a mathematical programming model in Refs. [19–22].

Arif et al. developed a two-stage optimization model for power management in distributed generation systems formulated as a mixed-integer linear program (MILP). The objective function of the first stage is the minimization of the distance between the depot in each cluster and damaged component of them. In the second stage of this model, the picked-up loads are maximized, and the repair time is minimized considering network operation, repair crew, and resource constraints [23]. Chen et al. expanded a sequential service restoration (SSR) model to generate restoration solutions for distribution systems in the event of large-scale power outages. This model maximizes the restored energy over time, considering system operation, connectivity, topology, and sequencing constraints with a MILP formulation [24]. Ding et al. also formulated the resilient distribution system by sectionalizing switches of systems. The objective function maximizes the total weighted sum of loads picked up after natural disasters on a mixed-integer linear programming with operation and topology constraints [25]. Nezamoddini et al. developed an optimization model as a mixed-integer linear programming (MILP) problem to determine the optimal investment decision (without considering the generation costs in the objective function) for the resilient design of the transmission systems against attacks. They measured the damage of the physical attacks in terms of the load curtailment [20].

Some authors developed an optimization model of energy resilience in multiple levels or stages. For example, Manshadi and Khodayar presented a mixed integer bi-level linear programming model for calculating the vulnerability of multiple energy carriers (electricity and natural gas) micro-grids against various interdictions to increase the resilience of energy supply and decrease the operation cost [26]. Yuan et al. also solved a resilient distribution network planning problem (RDNP) to organize the reinforcing and distributed generation resources. They developed a two-stage robust optimization model to minimize the system damage. The objective is maximizing the damage through a max-min bi-level game after the network planning decision [27]. Fang and Sansavini formulated a min-max-min model which implements the planner-attacker-defender model. The model objective functions were minimization of the total cost, maximization of system disruptions, and minimization of system performance loss after the attack. They solved this model as a three-level mixed-integer program (TLMIP) [28].

The typical bottom-up approach investigates rich details of technologies and emphasizes how several individual energy technologies can be used in each energy level [29,30]. To our knowledge, the only model that includes a bottom-up framework at the macro level was performed by Uemichi et al. [21]. However, their model calculated power generation systems resilience but did not consider fundamental energy system components in the long term. Therefore, their model can only investigate one energy carrier but would not analyze the role of fuel switching in enhancing the system resilience. Thus, no integrated framework considering all critical terms in energy system resilience faced to HILP events exists. This paper presents a novel long-term bottom-up-based mathematical framework for evaluating the resilience of energy systems against a HILP disruptive event resulting from climate change to overcome the drawbacks of the mentioned models.

The present paper focuses on developing a long-term optimization framework for evaluating the energy system resilience as a vital CI system against HILP caused by climate change. The main contributions of this research are: (1) calculating the vulnerability of an energy system against HILP climate change events based on energy resilience, (2) developing a two-stage optimization model to evaluate the resilience for a long-term energy planning considering economic, technical, and environmental features, parameter and constrain sets in the supply system, (3) designing the structure matrix (SM) to identify the interactions between the system and the vulnerable points for each HILP event resulted by climate change (4) providing a solution algorithm that allows trade-offs between resilience and economic objectives, and (5) applying the proposed model to a case study for reconfiguring the capability of an energy system to enhance system resilience.

The remainder of this paper is organized as follows. Section 2 defines the energy system resilience, whereas section 3 describes the conceptual framework of the model and proposes a detailed formulation of the two-stage model for the optimal total cost energy system under a HILP event resulting from climate change. Then, the solution method is introduced.

2. Energy system resilience

Despite extensive research on resilience, the concept of energy system resilience is still in its infancy. As a technical concept, resilience is a multifaceted capability of a complex system, including anticipating, avoiding, absorbing, adapting to, and recovering from disruptions [31,32]. It has been discussed, measured, and modeled in a variety of perspectives comprising social science [33], ecological [34], economic [35], and engineering [36]. As a branch of engineering resilience, energy system resilience is defined as actions taken following a disruptive event rather than before a disaster. This concept is shown in Fig. 1. The total future energy supply is significantly increased because of increasing the population growth and economic development under normal conditions (the red line) [37,38]. Anticipation, resistance, absorption, adaptation, and recovery from these events are prominent features of energy resilience to the exposure of a HILP, according to the Intergovernmental Panel on Climate Change (IPCC) report [39]. Avoiding the disruption of a system before the disruptive event by anticipation is the ‘safe-to-fail’ strategy (presented against ‘fail-safe’ (conventional risk management strategy) by Ahern [40]) which can minimize the energy system failures by predictive capabilities under HILP events [12]. Resistance focuses on absorbing HILP events, providing protection and robust energy systems, and adopting with (adjusting to) abnormal conditions [31,41,42]. Finally, a resilient energy system should demonstrate high recovery capabilities to restore the distorted infrastructures and damaged components and technologies duration of the impacts caused by HILP events and the dynamic characteristic of the energy system [43,44].

If a HILP event occurs in t_1 , the total energy supply is decreased until restoring time (t_2). This trend will continue until the system achieves a stable condition again. Thus, we identify four states associated with a disruptive event; stable original state ($t_0 - t_1$), disrupted state ($t_1 - t_2$),

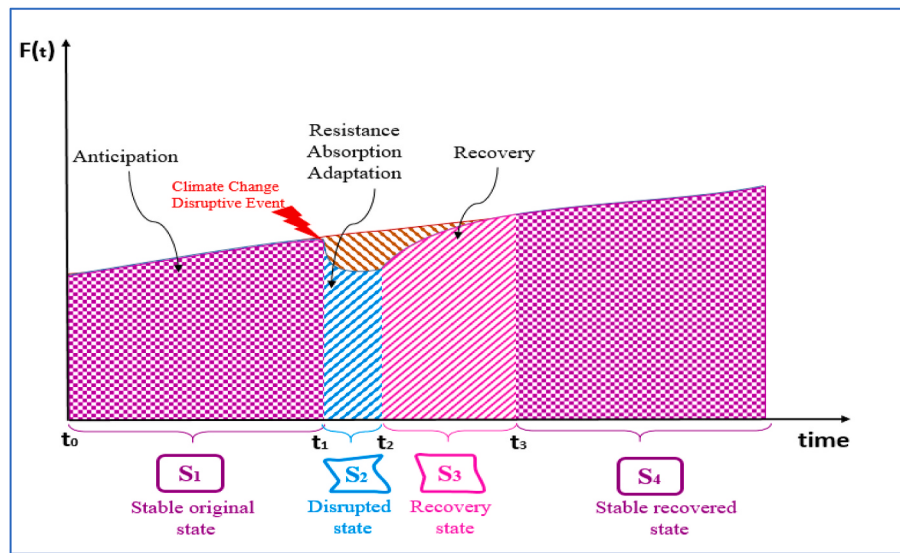


Fig. 1. Conceptual energy resilience associated with a HILP event resulting from climate change.

recovery state ($t_2 - t_3$) and stable state after recovery ($t_3 - t_n$). Resilience for energy systems can also be defined as the ability of an energy system to minimize disruptions to energy service by anticipating, resisting, absorbing, adapting to, and recovering from a disruptive event. The anticipation of a disruptive event can be considered in the original stable state, resistance, absorption, and adaption of energy systems can be measured in the disrupted state, and recovery of the disrupted system is determined in the recovery state [45,46].

3. Model description

An energy system is organized to meet the demand for energy services, and since a HILP disruption event resulting from climate change is an inevitable part of socio-economic systems, examining energy system resilience is essential. The resiliency of each energy system is calculated based on changes in the level of system performance after the occurrence of a HILP disruptive event compared to the optimal performance of the system before the disturbance. As seen in Fig. 1, the dynamic behavior of the energy system after a HILP disruptive event can be investigated over four-time intervals. In the event of an impairment, changes are made to the optimal dynamic behavior of the system, which can be investigated in these four time periods:

1 Stable original state: The optimal system performance ($F(t)| t_0 < t < t_1$) before a HILP disruptive event in which t_1 will be considered the starting time point of the HILP disruption. The system is assumed to be in optimum condition prior to this time point and is therefore consistent with the activity level obtained from the optimal models.

2 Disrupted state: The impact propagation phase ($t_1 < t < t_2$) in which damages due to the HILP event occur and lead to a reduction or even halt of the operation of the existing system. Considering this section, both the pattern of activity levels degradation and impact propagation time are technical issues depending on the type of system operation, the system design, and the severity of the HILP disruption. Therefore, calculating the time and pattern of activity reductions requires analyzing disturbances or examining historical data on the extent to which past events affect the existing systems. Hence, it should be given to the system as an exogenous pattern for any possible disturbances to existing and new systems.

3 Recovery state: The system recovery stage, expanded from t_2 to t_3 in Fig. 1, having a pattern depending on the type of disruption and the extent of its destruction in each system's component. Therefore, the duration of the repairs and the gradual increase in the performance

level of the system ($F(t)$) should be exogenously added to the proposed model for each of the technologies in the energy supply system.

4 Stable recovered state: The normal operation stage of the system is after the recovery period. This interval time ($t > t_3$), as seen in Fig. 1, is the stage at which the level of system activity returns to the optimal level based on the solution of the classic model and regardless of the disruption event.

Capacity variables for installing new technologies and combining high-efficiency technologies to reduce fossil fuel resource extraction and environmental destruction, as well as variation in the primary energy composition for the expansion of the system's flexibility, are modeled in the proposed method. Therefore, the model can develop a system by adopting various strategies for structural change in the years to come. In the disruptive environmental event affecting the system performance, the overall reduction of system activity level and the recovery time are minimized. Therefore, the overall system resilience index is maintained at a desirable level with an optimization two-stage model. The proposed conceptual model will be developed based on energy supplier behavior and the effects of resilience on its behavior. The proposed model is a two-stage optimization model with an intermediate stage for the HILP disturbance propagation, according to Fig. 2.

Nonlinear programming creates a wide-ranging paradigm for many problems in the social and economic sciences. The uncertainty caused by climate change and the impact of extreme weather events is nonlinear and nonlinear programming fit better the real world in analyzing energy resilience. Nevertheless, unlike LP, there is no universally applicable algorithm, and this programming cannot be easily solved by existing software. Most importantly, by solving LP models, a globally optimal solution can be obtained in the feasible region with a better objective value than other feasible solutions. In contrast, NLP models may have various local optimal solutions in the feasible region. Thus, LP is a large field of optimization for numerous reasons. Hence, the developed model is structured by LP programming, and in the disrupted state of the system, for nonlinear $d_p(t)$, a good trade-off is to resort to piece-wise linear approximations in the different range. Thus, the formulated multi-stage resilience energy model is proposed as an LP program. This model optimizes the present value of the total costs of capacity expansion of an energy system and energy needed but not supplied (ENNS) cost under a HILP disruptive event resulting from climate change.

In the first stage, the energy system optimization model will be developed based on the theoretical concept of classical microeconomics

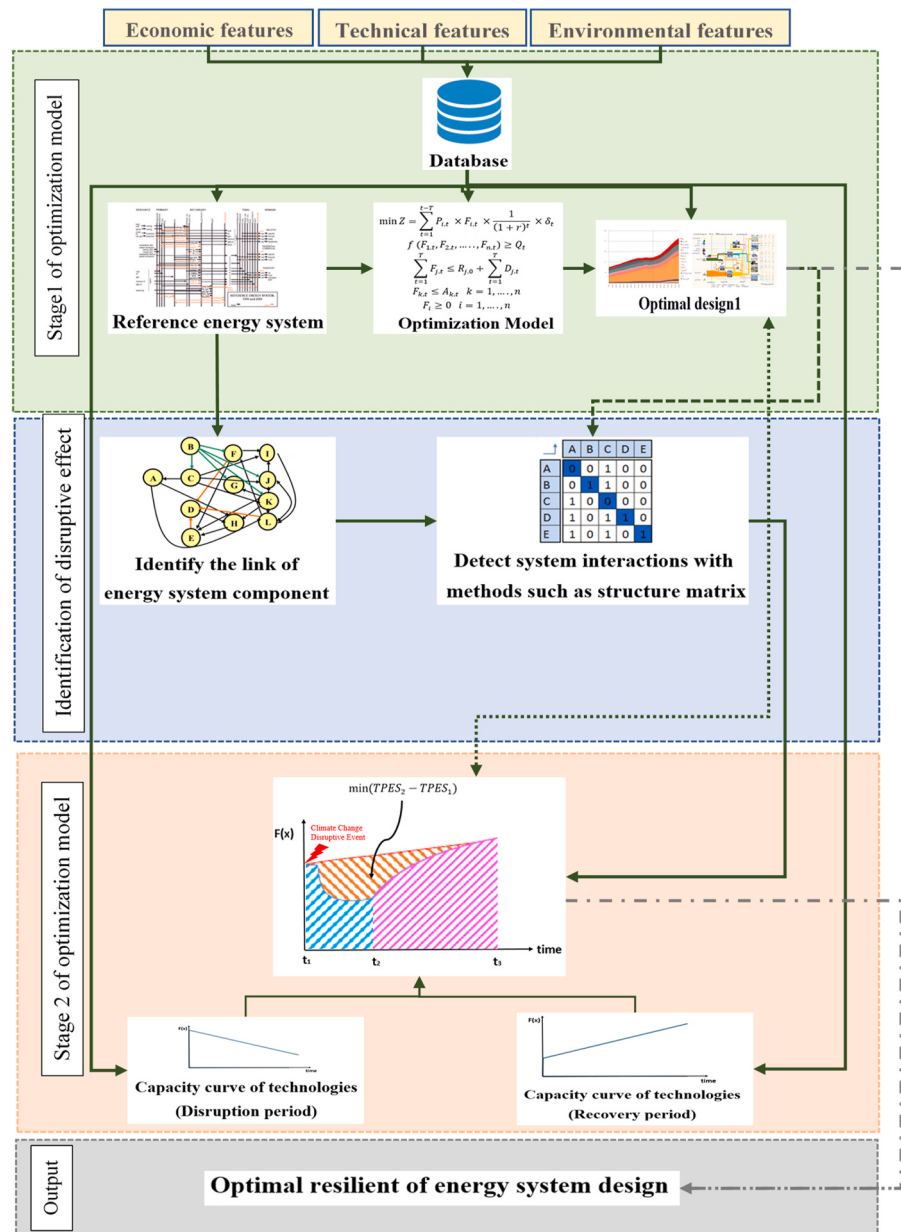


Fig. 2. Overview of the integrating modeling framework.

in which the energy supplier is an organized firm active in the energy market. For this purpose, the reference energy system (RES) is first drawn to depict fundamental relationships among the stocks, flows, technologies, and different levels of the energy system. Then, an optimization model is developed based upon RES, cost issues, capacity factor, efficiency, operation modes, physical limitations, and environmental constraints. In this period, the activity levels of the considered energy system and the GHG production are calculated from the optimal model by minimizing the total cost objective function.

In the intermediate stage, the link between a HILP disruptive event and the considered energy system is identified by a structure matrix (SM). Here the connections between the energy system's components are determined based on the developed RES in the first stage, and the structure matrix is developed for selected technologies in the first stage optimization model.

In the second stage, the amount of energy needed but not supplied (ENNS) is calculated using an optimization model, activity patterns of the damaged technologies regarding SM in the intermediate stage, and the recovery activity levels with capacity curves. Finally, the resiliency

of the energy system is maximized by minimizing the difference of the total primary energy supply (TPES) in the first and second stages.

3.1. First stage of the optimization model

In the first stage, an optimization model is developed, as a programming problem, by organizing technologies to extract, process, convert and distribute the energy carriers to end-users regarding RES (as a conceptual model) based on the ESM¹ model.

As a classic energy model, this model is defined by an objective function and a set of constraints. The objective function of the present deterministic energy system model is the minimization of the discounted total cost of energy (DTCE), which may be presented according to the following relationship and expanded in Table 1.

$$Z = \min (\bar{K} + \bar{M} + \bar{C} + \bar{R} + \bar{E}) \quad (1)$$

¹ Energy System Model.

Table 1

Underlying formulations of the first stage model.

Equations	Remarks
a. Sets of constraints	
1. Demand constraints	
1.1. $\sum_{k=1}^m \sum_{t=1}^n F_{kjilt} \times \eta_{kjilt} \geq D_{jilt} \times \alpha_{jil}$	$\forall \tau \in \text{demand technologies} \& \forall t \in \text{planning years}$
1.2. $\frac{F_{kjilt} \times \eta_{kjilt}}{\Delta l} - \sum_{\omega=t-PL}^t Y_{kjil\omega} \times PF_{kjilt} \leq \sum_{\theta=b-(PL-t)}^b H_{kjil\theta} \times PF_{kjilt}$	$\forall \tau \in \text{demand technologies} \& \forall 1 < \omega < t \& \forall t \in \text{planning years}$
2. Distribution constraints	
2.1. $\sum_{\delta=1}^{n'} T_{k\delta kl\tau} \times \eta'_{k\delta kl\tau} = \sum_{\tau=1}^n T_{k\tau kl\tau}$	$\forall \delta \in \text{distribution level technologies} \& \forall t \in \text{planning years} \&$ $\forall \tau \in \text{demand technologies}$
2.2. $\frac{T_{k\delta kl\tau} \times \eta'_{k\delta kl\tau}}{\Delta l} - \sum_{\omega=t-PL}^t Y_{k\delta kl\omega} \times PF_{k\delta kl\omega} \leq \sum_{\theta=b-(PL-t)}^b H_{k\delta kl\theta} \times PF_{k\delta kl\theta}$	$\forall \delta \in \text{distribution level technologies} \& \forall 1 < \omega < t \& \forall t \in \text{planning years}$
3. Conversion constraints	
3.1. $\sum_{e=1}^{m''} \sum_{\mu=1}^{n''} U_{epklt} \times \eta''_{epklt} = \sum_{\delta=1}^{n'} T_{k\delta kl\tau}$	$\forall \mu \in \text{conversion technologies} \& \forall t \in \text{planning years}$
3.2. $\frac{U_{epklt} \times \eta''_{epklt}}{\Delta l} - \sum_{\omega=t-PL}^t Y_{epk\omega} \times PF_{epk\omega} \leq \sum_{\theta=b-(PL-t)}^b H_{epkl\theta} \times PF_{epkl\theta}$	$\forall \mu \in \text{conversion technologies} \& \forall 1 < \omega < t \& \forall t \in \text{planning years}$
4. Process constraints	
4.1. $\sum_{e=1}^{m'''} \sum_{\gamma=1}^{n'''} P_{oyelt} \times \eta'''_{oyelt} = \sum_{\mu=1}^{n''} U_{epklt}$	$\forall \gamma \in \text{conversion technologies} \& \forall t \in \text{planning years}$
4.2. $\frac{P_{oyelt} \times \eta'''_{oyelt}}{\Delta l} - \sum_{\omega=t-PL}^t Y_{oyel\omega} \times PF_{oyel\omega} \leq \sum_{\theta=b-(PL-t)}^b H_{oyel\theta} \times PF_{oyel\theta}$	$\forall \gamma \in \text{conversion technologies} \& \forall 1 < \omega < t \& \forall t \in \text{planning years}$
5. Resources constraints	
5.1. $\sum_{t=1}^T \sum_{l=1}^v \sum_{\gamma=1}^{n'''} P_{oylt} \leq \sum_{t=1}^T R_{ot} + \sum_{l=1}^v \sum_{t=1}^T I_{olt}$	$\forall o \in \text{energy carriers} \& \forall t \in \text{planning years} \& \forall l \in \text{load zones}$
6. Use of economic resource constraint	
6.1. $B_{ot} = \sum_{\rho} b_{opt} \times X_{pt} \leq \beta_{ot}$	$\forall o \in \text{energy carriers} \& \forall \rho \in \text{control volumes} (\text{ie. technology})$
7. Environment constraint	
7.1. $P_{at} = \sum_{\rho} p_{apt} \times X_{pt} \leq \psi_{at}$	$\forall a \in \text{pollutants} \& \forall \rho \in \text{control volumes}$
8. Bound on flow constraint	
8.1. $X_{pt} \leq \lambda_{pt}$ \geq	$\forall \rho \in \text{control volumes} \& \forall t \in \text{planning years}$ This equation is added due to physical or institutional constraints (as social or political limitations)
b. Objective function	
$Z = \min(\bar{K} + \bar{M} + \bar{C} + \bar{R} + \bar{E})$	
$\bar{K} = \sum_{t=1}^T \sum_{\varphi} \sum_{\tau} \left[\frac{k_{\varphi rt} \times Y_{\varphi rt}}{(1+r_t)^t} \right]$	Capital cost $\forall \varphi \in \text{sub-systems} \& \forall t \in \text{planning years} \& \forall \tau \in \text{control volumes}$

(continued on next page)

Table 1 (continued)

Equations	Remarks
$\bar{M} = \sum_{t=1}^T \sum_{\varphi} \sum_{\tau} \left[\frac{m_{\varphi t} \times [\sum_{\omega=1}^{\ell} Y_{\varphi \omega t} + H_{\varphi t}]}{(1+r_t)^t} \right]$	Maintenance cost $\forall \varphi \in \text{sub-systems} \& \forall t \in \text{planning years} \& \forall \tau \in \text{control volumes}$
$\bar{C} = \sum_{t=1}^T \sum_{\varphi} \sum_{\tau} \sum_l \left[\frac{c_{\varphi l t} \times X_{\varphi \omega t} \times \eta_{\varphi t}}{(1+r_t)^t} \right]$	Operation cost $\forall \varphi \in \text{sub-systems} \& \forall t \in \text{planning years} \& \forall \tau \in \text{control volumes.} \& \forall l \in \text{load zones}$
$\bar{R} = \sum_{t=1}^T \sum_{\varphi} \sum_l \left[\frac{v_{\varphi l t} \times R_{\varphi l t}}{(1+r_t)^t} \right]$	Resource cost $\forall \varphi \in \text{sub-systems} \& \forall t \in \text{planning years} \& \forall \tau \in \text{control volumes}$
$\bar{E} = \sum_{t=1}^T \sum_{\varphi} \sum_{\tau} \sum_k \sum_l \left[\frac{e_{k l t} \times \gamma_{\varphi k t} \times X_{\varphi \omega t} \times \eta_{\varphi t}}{(1+r_t)^t} \right]$	External cost $\forall \varphi \in \text{sub-systems} \& \forall t \in \text{planning years} \& \forall \tau \in \text{control volumes} \& \forall l \in \text{load zones} \& \forall k \in \text{pollutants}$

where Z is the objective function, \bar{K} indicates the discounted capital cost, \bar{M} is the discounted maintenance cost, \bar{C} represents the discounted operation cost, \bar{R} is the discounted resource/fuel cost, and \bar{E} denotes the discounted external cost such as environment cost. This objective function is determined by deploying fundamental relations and set constraints presented in Table 1. However, these constraints may not be limited to what is listed here, and an additional set of constraints such as reliability consideration of power plants, market share of a specific technology, and bounds on flow or capacities could be added to the present model.

3.1.1. Intermediate stage

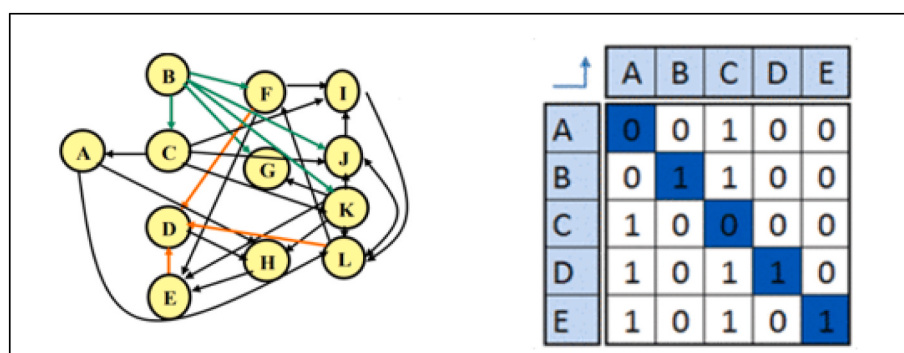
At this stage, the energy system actors are identified based on drawings on RES and the model database for organizing the Structure Matrix of the system (SM). The SM is a suitable tool for network modeling used in this research to identify inter-system interactions and susceptible parameters of system failure. The structure matrix is designed to identify the interactions between the system and the vulnerable points for each HILP event resulting from climate change. As shown in Fig. 3, this matrix is a square matrix that the energy system components are its row and column components, and the impact of the HILP on each component is shown by zero and one. If the climate change disruption affects one or more energy system components, all relevant components are assigned one based on system interaction. Otherwise, the corresponding cell is assigned zero. It should be noted that all existing and new-build technologies identified in RES, along with system components interactions, should be presented in this matrix. The purpose of completing this matrix is to determine the severity of the impact of the destructive events corresponding to the different components.

3.1.2. Second stage of the optimization model

After modeling the energy supply system in the original stable state, rendering Fig. 1, and obtaining the optimum point to supply of useful energy demand under the conditions of the lowest long-term cost of the system, it is necessary to make some changes in this classical model that can be adapted to disrupted and recovery states. Therefore, at this stage, we seek to exert some changes in the model equations of the energy supply system that can provide optimal system conditions and technology selection patterns after HILP disruptive events. Hence, the second stage model is the same first-stage model with the following changes.

3.1.2.1. Step 1: Relaxing the energy demand constraint set. In the first step, it is essential to note that, unlike the classical model, which always seeks to provide the full of helpful energy demand for all planning years, in the present state, part of the final energy demand during the critical period may not be met because of HILP disruptive events in the disruption year and some years after that. Obviously, in this state, the energy supply system will not fully supply energy demand for a short period, but the model is trying to minimize this period in the shortest possible time (minimize recovery time).

To accomplish this, and since the objective function of the first-stage model is a function of the total cost, it is suggested to minimize the cost of energy needed but not supplied (ENNS) during the critical period, which is added to objective function as a penalty cost by Equations (19)–(21). The ENNS is estimated based on total primary energy calculated by the first stage model and identifying affected technologies by SM in the intermediate stage. This cost, such as investment and operational costs, should be discounted to the base year in addition to the objective

**Fig. 3.** A typical structure matrix (SM).

function. For this aim, Equation (2) is relaxed for all planning time points, and Equations (19) and (20) are added to the second stage model.

$$\text{penalty}_{jilt} = c_{ji} \times \left(U_{jilt} \times \alpha_{jil} - \sum_{k=1}^m \sum_{\tau=1}^n F_{k\tau jilt} \times \eta_{k\tau jil} \right) \quad (19)$$

The penalty cost of ENNS should be discounted as Equation (20) for adding to Equation (21).

$$z_{ENNS} = \sum_t \sum_l \sum_i \sum_j \left[\frac{\text{penalty}_{jilt}}{(1 + r_t)^t} \right] \quad (20)$$

$$Z = \bar{K} + \bar{M} + \bar{C} + \bar{R} + \dots + \sigma \times z_{ENNS} \quad (21)$$

It is important to note that the choice of the exogenous coefficient c_{ji} in Equation (19) must be realistic and large enough that the model always meets the maximum demand in disruption conditions. At the same time, this change avoids the infeasibility of the model in disrupted and recovery states. The calculation of the c_{ji} coefficient should be done sorting the energy demand carriers separately, and the amount of their failure penalty is based on energy system realities or critical events analysis. For example, realistic estimates of these parameters can be obtained by analyzing the damages caused by power or natural gas outages due to floods, earthquakes, and HILP disruptive events resulting from climate change and can be extrapolated to different scenarios in the future years.

3.1.2.2. Step2: Applying disruption propagation and system recovery patterns. In the second step of this stage, and in addition to the change in the objective function of the proposed model relative to the stable state, changes in the set of technical constraints of the energy system are necessary. These changes should influence the parameters related to disruptive event-affecting technologies (i.e., SM) in the following disruptive propagation and recovery years. As mentioned earlier, each energy system undergoing HILP events has three states after the disruptive event; disruption propagation modes, system recovery, and recovered stable state. Therefore, these developments will be conceivable for any technologies in the reference energy system and non-zero in the structure matrix. Thus, if technology i (i.e., a refinery or pipeline) is affected by a HILP event, all or some of its parameters will change in each of these periods. These parameters include capacity, efficiency, and investment costs, which form the major part of the technical coefficients of constraints sets in mathematical modeling. For example, suppose event-affected technology is a refinery with a capacity of 360,000 bbl./day, which be fully shutdown after a HILP event, and historical analysis

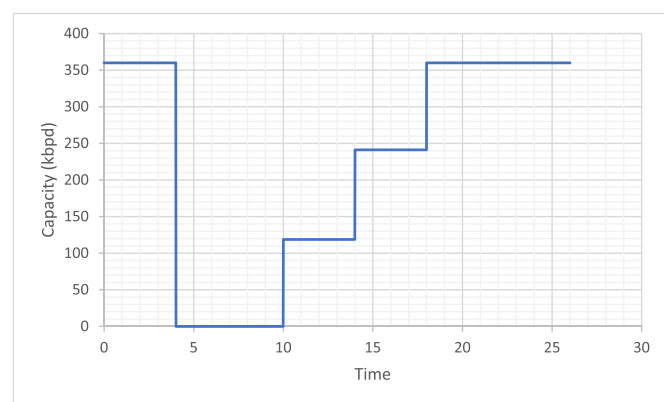


Fig. 4. Changes in the capacity of a typical refinery after disruption and recovery.

of past events shows that the capacity of the refinery returns to nominal capacity in three steps and then will enter equilibrium after recovery according to Fig. 4.

Based on the above generalization, a function can be proposed as a disruption-recovery pattern for each of the RES technologies, the value of which in the normal operating conditions of each component and the stable recovered conditions after disruption is one. Furthermore, during the disruption and recovery period of the energy system, the system operating capacity has values of zero (lack of system performance) or less than one (performance below capacity).

If $dp(t)$ is an example of this disturbance pattern function assuming a HILP event at $t = 0$, it can be considered for various patterns, such as stepwise, linear, and exponential, according to Fig. 5. The choice of each pattern will depend on the analysis of the historical events and how the system is configured technically.

If the technological capacity is affected by the HILP event, the capacity constraint sets are changed from Equations ((3), (5), (7) and (9)) to Equations (22)–(25) respectively. In these equations, T_1 is the time of occurring the disturbance event. Therefore, the disruption and recovery pattern can affect both the existing capacities and the new capacities constructed by the model, and this model creates a new scale for the Plant Factor coefficient of equations.

$$\frac{F_{krjilt} \times \eta_{krjil}}{\Delta t} - \sum_{\omega=t-PL}^t dp(t-T_0) \times Y_{krjilo} \times PF_{krjilt} \leq \sum_{\theta=b-(PL-t)}^b dp(t-T_0) \times H_{krjil\theta} \times PF_{krjilt} \quad (22)$$

$$\frac{T_{k\delta klt} \times \eta'_{k\delta klt}}{\Delta t} - \sum_{\omega=t-PL}^t dp(t-T_0) \times Y_{k\delta klo} \times PF_{k\delta klt} \leq \sum_{\theta=b-(PL-t)}^b dp(t-T_0) \times H_{k\delta klt\theta} \times PF_{k\delta klt} \quad (23)$$

$$\frac{U_{epklt} \times \eta''_{epklt}}{\Delta t} - \sum_{\omega=t-PL}^t dp(t-T_0) \times Y_{epklo} \times PF_{epklt} \leq \sum_{\theta=b-(PL-t)}^b dp(t-T_0) \times H_{epklt\theta} \times PF_{epklt} \quad (24)$$

$$\frac{P_{oyelt} \times \eta'''_{oyelt}}{\Delta t} - \sum_{\omega=t-PL}^t dp(t-T_0) \times Y_{oyelt} \times PF_{oyelt} \leq \sum_{\theta=b-(PL-t)}^b dp(t-T_0) \times H_{oyelt\theta} \times PF_{oyelt} \quad (25)$$

3.2. Solution strategy

The total objective function referring to the minimization of DTCE in the first stage and its total primary energy supply ($TPES_1$) also total primary energy supply in the modified second stage model ($TPES_2$) are solved sequentially and iteratively to obtain the optimum amount of the total supply quantities in each time with calculating the energy resilience index (equation (26)). Therefore, the overall objective function of the proposed system model is determined by Equation (27). If the considering level is the intermediate or final level, TPES will be replaced by total secondary energy supply (TSES) and total final energy supply (TFES), respectively.

$$R_{index} = (TPES_1 - TPES_2) \quad \& \quad 0 < R_{index} < TPES_1 \quad (26)$$

$$\max (R) = \min (TPES_1 - TPES_2) \quad (27)$$

Therefore, the developed model is a two-stage model modeled as an integrated considering objective function and all constraint sets in each sub-model. This two-stage model is solved using the following algorithm (Fig. 6).

3.3. Indicators

In addition to the resilience index, three indicators are applied for considering the vulnerability of energy systems against HILP events: robustness, recovery time, and readjust-ability. Robustness is a characteristic of an energy system during a disruption event that shows how a system can absorb turbulence and continue to supply the energy demand. This indicator is determined as Equation (28) [47]. Recovery time is another indicator that presents the speed of the recovery process and is calculated as Equation (29). Readjust-ability represents the capability of the system to adapt to a situation in which it cannot absorb stress and is complementary to mitigation. This indicator is evaluated by Equation (30) [47].

$$\text{Robustness}_{index} = \frac{2}{1 + \exp\left(\frac{F_d - F_d}{F_d}\right)} \quad (28)$$

$$\text{Recoverytime}_{index} = t_F - t_d \quad (29)$$

$$\text{Readjust-ability}_{index} = \frac{F_F}{F_s} \quad (30)$$

4. Application to a case study

UTOPIA as a typical example used in some models as MARKAL [48] and OSeMOSYS [49] is applied to verify the proposed model (developed

in GAMS software), and the results are shown in Appendix 1. Also, we use Atlantis, a fictitious country that shares features of the energy system in both a developing and a developed country, organized by the UN to train Government staff in energy systems modeling and planning practices [50]. There are four energy levels in Atlantis; Final energy, Tertiary, Secondary and primary. The energy system is developed for supplying electricity demand in industry, household, transportation, and services sections. The reference energy system of Atlantis is presented in Fig. 7. The yearly demand is split through the year to shape the demand profile, and the year is split into six time-slices. Coal, uranium, heavy fuel oil, gasoline, diesel, natural gas, solar, and wind are energy resources, and water is non-energy resources imported in Atlantis. Primary energy carriers were historically converted in five power plant types to supply energy demand; natural gas-fired Single Cycle Steam Turbine (PP1), diesel-fed Open Cycle Gas Turbine (PP2), coal-based Integrated Gasification Combined Cycle facility (PP3), heavy fuel oil-fired Single Cycle Steam Turbine (PP4) and large hydropower plant (PP5). Concentrated solar power plants (CSP), new Combined Cycle Power Plant running on natural gas (CCGT-NG), wind power plant (with 25% load factor), new nuclear power plant and grid-connected PV systems are added as control volumes in secondary energy level to meet electricity demand in future years. Distributed diesel generators, mini hydropower plants (less than 1 MW), and transmission technologies are the next energy level. Rooftop PV systems are another energy supply system that provides the energy needed in the residential sector.

5. Result and discussion

The original data set of Atlantis is available on GitHub [51], and the modeling period is 2014–2060. Four scenarios have been developed for considering the energy system resilience against HILP events caused by climate change; Business As Usual (BAU), No Adaptation Strategy (NAS), Business As Usual with Adaptation Strategy (BAUAS), and Renewable Target with Adaptation Strategy (RTAS). In the BAU scenario, the optimal pattern of the model has been determined without any disruption events; however, in two other scenarios, we have assumed a climate change event occurring in 2045. Indeed, in the first scenario, an optimal pattern is obtained from only the first stage of the model, and in the others, it is specified by the integrated model.

The model results show the optimal combination of technologies at the secondary level. Fig. 8 illustrates the energy production in power plants without any disruptions in the BAU scenario. The share of hydropower plants (Dam and Mini) in the total electricity generation mix is very significant, close to 65%, dropping to 46% in the end year. However, the share of the PV power plant is expected to increase about 8% (post-2050). Nuclear and wind power plants are also expected to play an essential role in the electricity generation mix during a period.

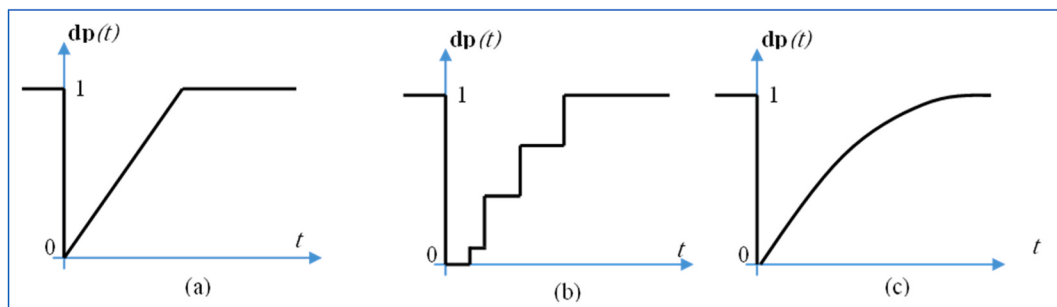


Fig. 5. Samples of linear (a), stepwise (2), and exponential (3) disturbance-recovery functions.

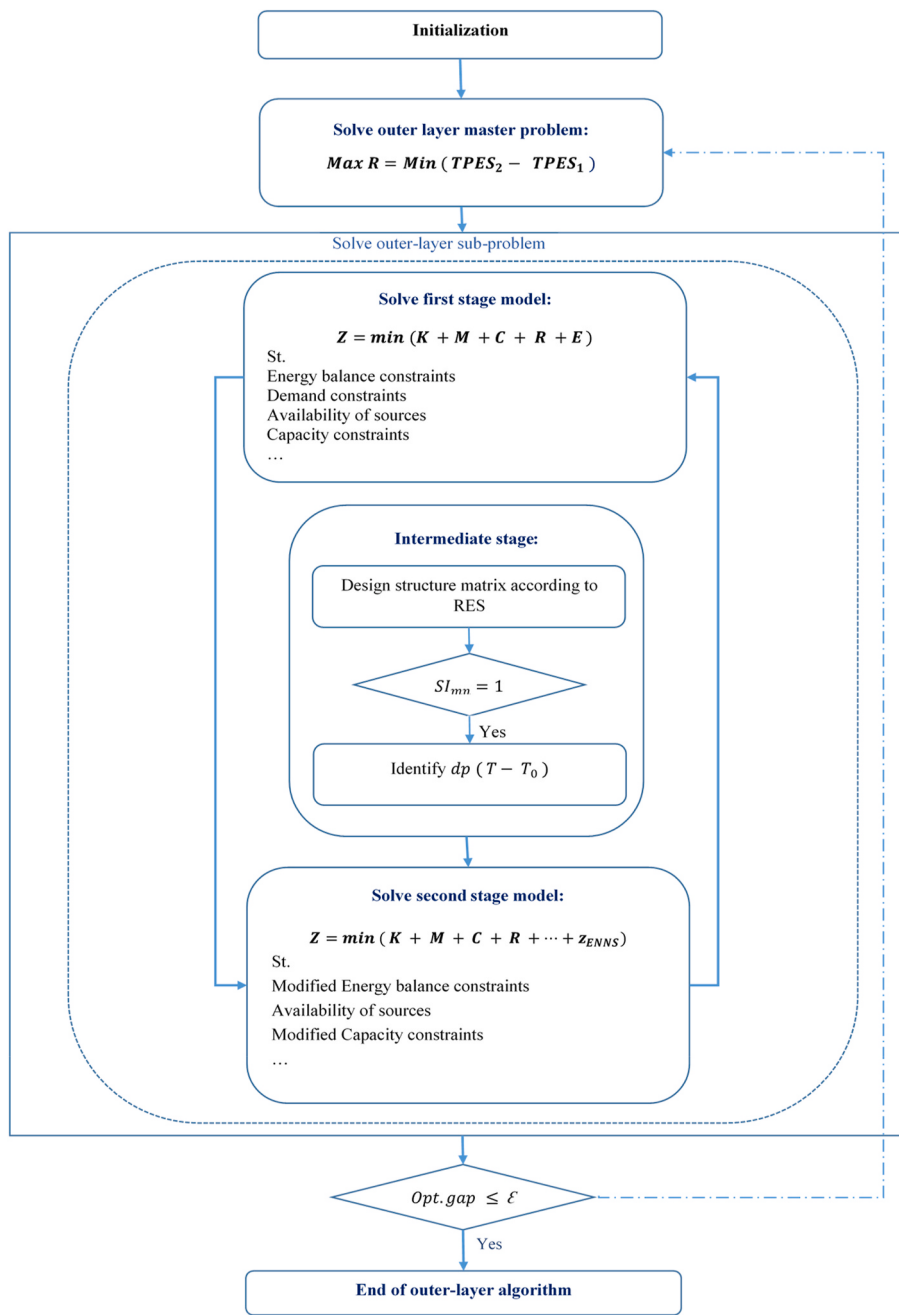
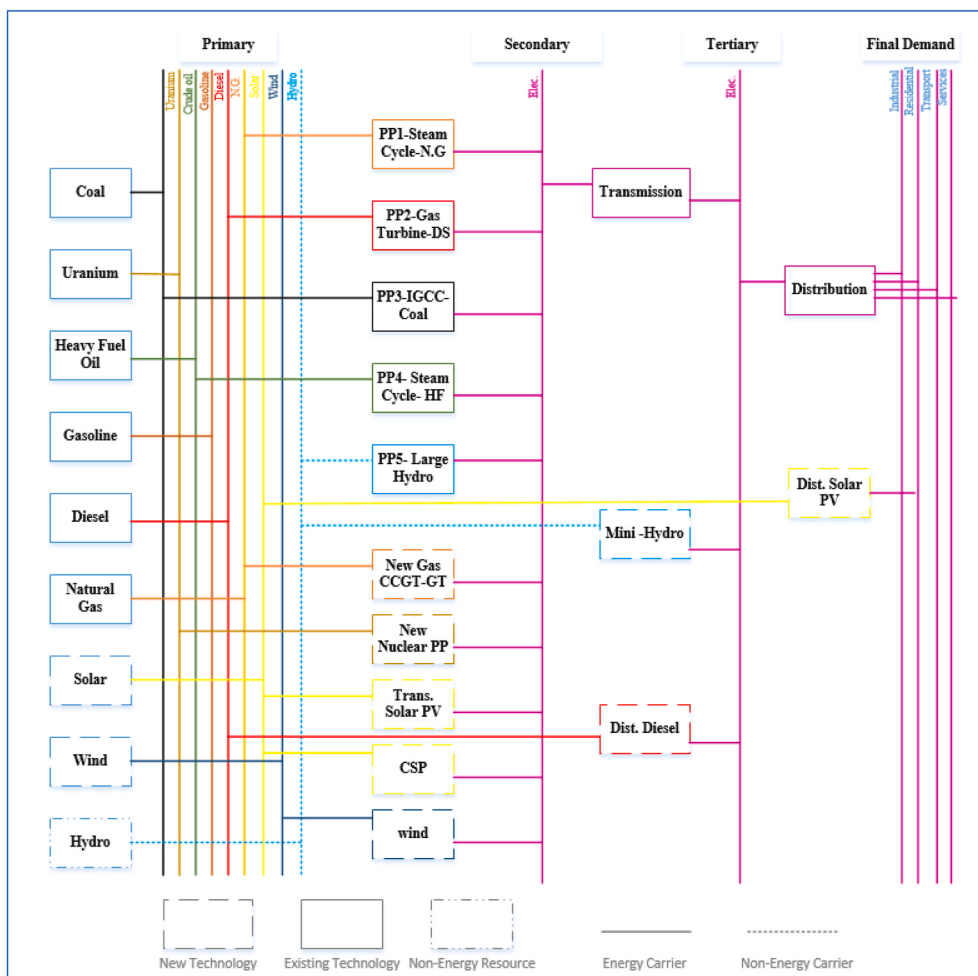
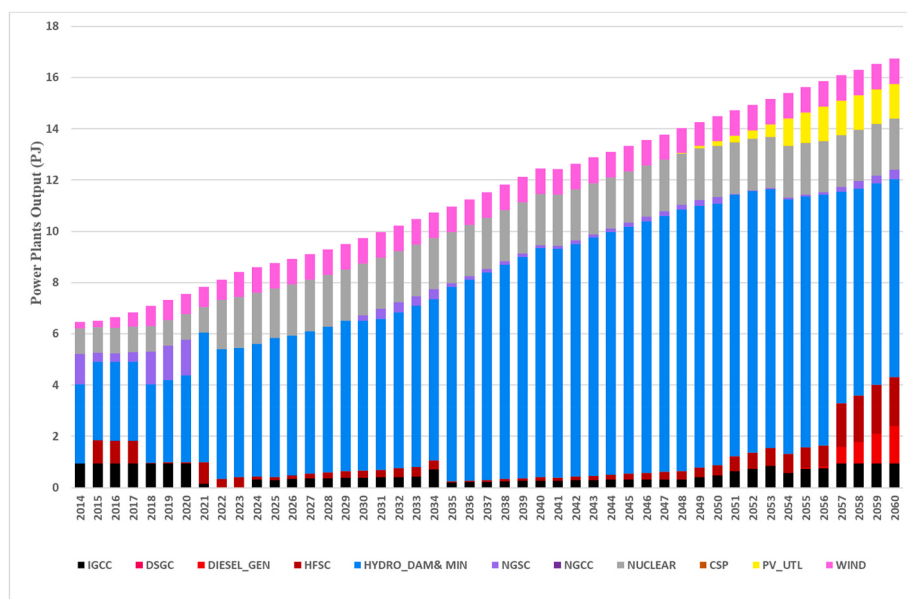


Fig. 6. Schematic algorithm for solving the integrated proposed framework.

For considering the climate change effect on RES technologies and energy flows, the structure matrix of Atlantis has been identified as Fig. 9. An increase in temperature and extreme temperatures are the main aspects of climate change as a HILP event that the impact of rising ambient air temperatures and changes in annual and seasonal precipitation will impact water supply and resource availability. This event's effects on other control volumes of energy systems and the interaction between different technologies and climate change were internalized by external costs, which gathered from Ref. [52] and added to the second stage of the model. Steam cycle-NG, gas turbine-DS, IGCC-coal, steam cycle-HF, large hydro, CCGT, nuclear power plant, trans solar, CSP,

wind, mini hydro, and solar are the leading technologies that climate change impacts, as shown in Fig. 9. On the other hand, for recognizing $dp(t)$, we used the results of Raj et al. [53] hydrologic model, which shows a decrease in annual hydropower generation for all climate change scenarios in 2045–2065, as demonstrated in Fig. 9. Hence, $e^{-0.074 t}$ and $0.7e^{0.063 t}$ are $dp(t)$ functions in the disruption and recovery functions.

We assumed the mentioned HILP occurred in 2045 and ran the model for NAS, BAUAS, and RTAS scenarios; the results are shown in Fig. 10a, b, and 10c respectively. In NAS, any adaptation actions do not happen, and the electricity generation mix is selected based on energy planning

**Fig. 7.** Atlantis reference energy system (RES).**Fig. 8.** Energy production in power plants of Atlantis in BAU scenario.

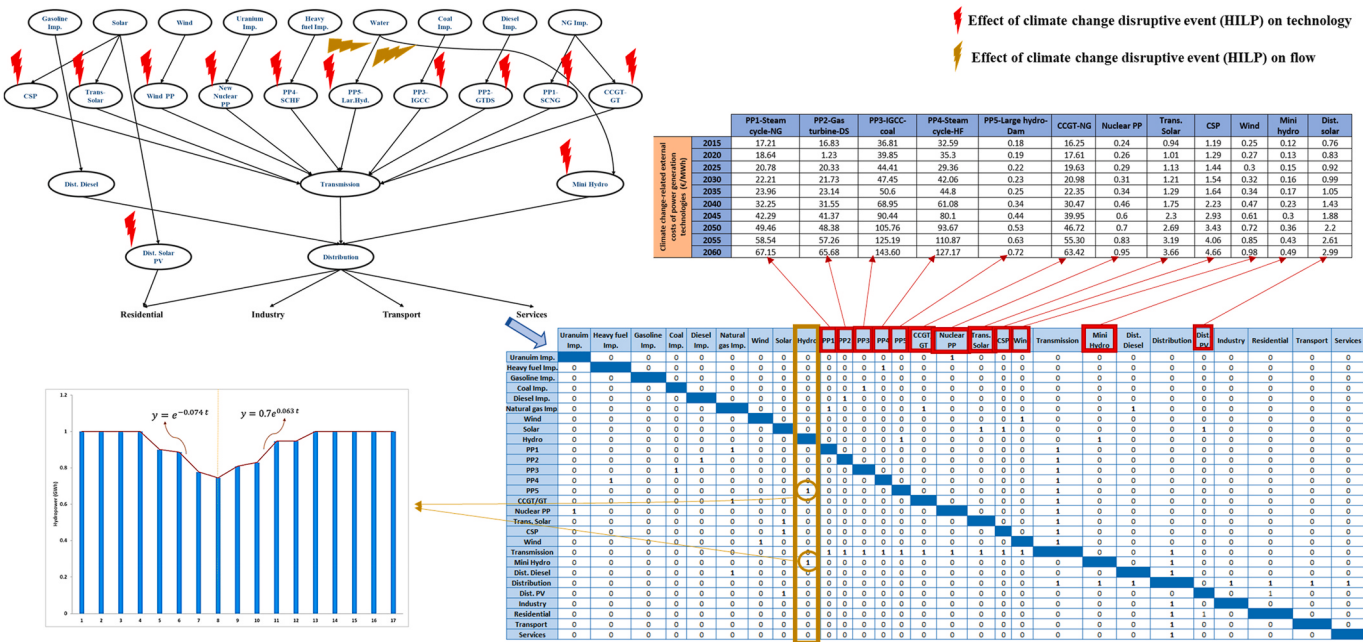


Fig. 9. Result of intermediate stage: Structure matrix of ATLANTIS and effects of HILP event on technologies and flows.

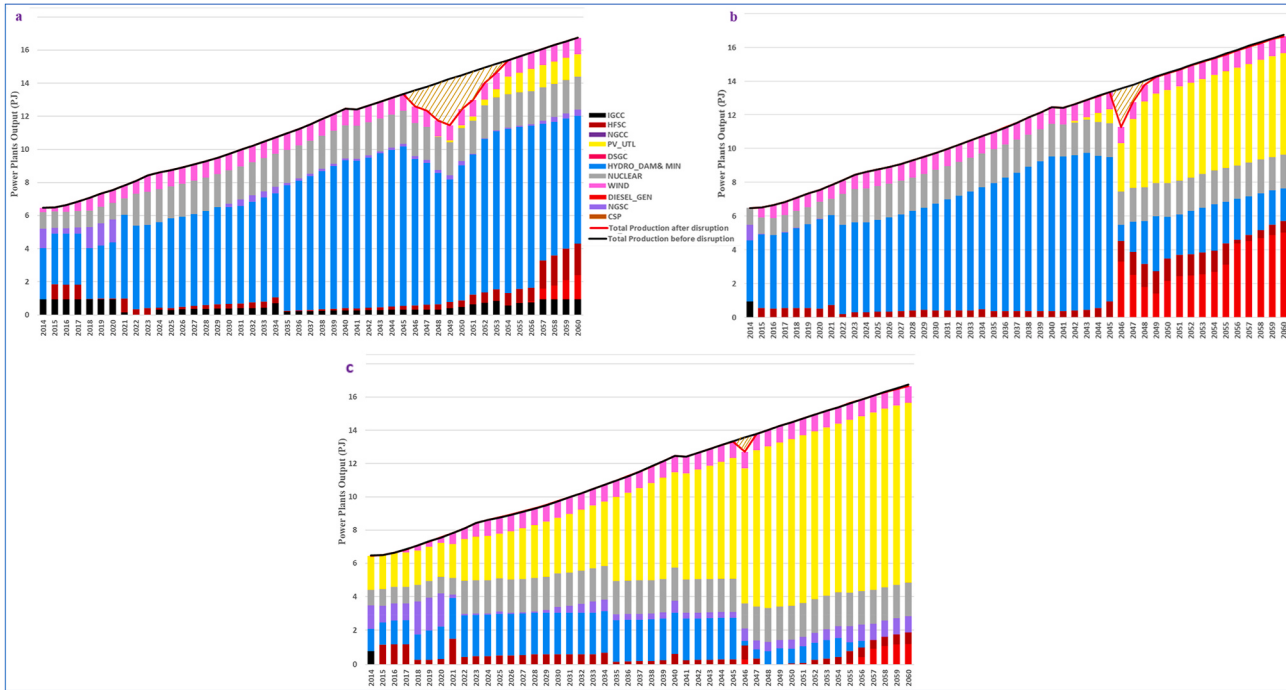


Fig. 10. a) Energy production in power plants of Atlantis in NAS scenario, b) Energy production in power plants of Atlantis in BAUAS scenario, c) Energy production in power plants of Atlantis in RTAS scenario. $\sigma = 1$

strategy ignoring resiliency. In this scenario, the resilience index is 12.7, and the Atlantis energy system is not robust since climate change impacts the annual useable capacity of hydropower that has the largest share of electricity generation. On the other hand, results demonstrate fuel switching from hydro and coal to solar in BAUAS and RTAS scenario as Fig. 10b and c, because of considered climate-change external cost

since the early year. The noteworthy point in comparing the three scenarios is that the years of system performance decline due to non-implementation of resilience policies are four years in the NAS scenario.

In comparison, in the two other scenarios, the system begins to recover performance in the first year after performance loss and improves the system. Also, the amount of unmet demand in the NAS

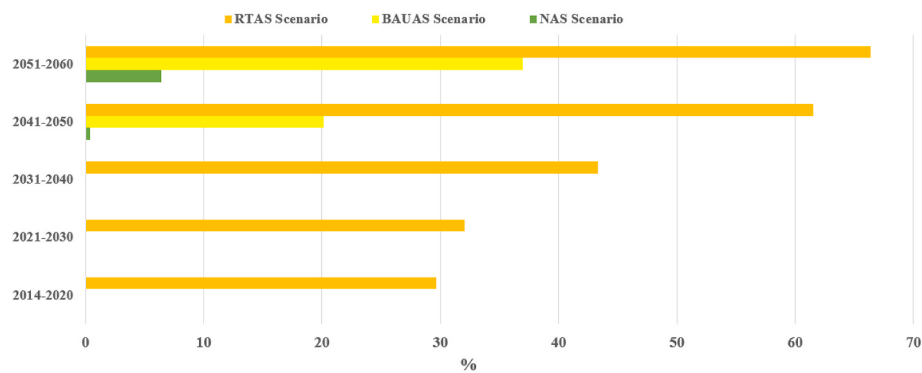


Fig. 11. The share of solar power plants out of the total primary energy supply in 10 years.

Table 2
Indicators in NAS, BAUAS and RTAS scenarios.

	robustness	recovery time	adjust-ability	R_{index}
NAS scenario	0.89	5 years	1	12.72
BAUAS scenario	0.91	3 years	1	3.32
RTAS scenario	0.97	1 year	1	0.86

scenario is much higher than the cumulative energy needed but not supplied in the other two scenarios. The share of the hydropower plant in the total electricity generation mix in RTAS is 19% (in the start year), dropping to 1% in the end year, and PV replaces hydropower; this value drops from 55% to 10% in the BAUAS. In the BAUAS scenario, the large part of the demand that is not met by the outflow of hydropower plants is supplied by diesel generators as a distributed system in the optimal system design mode. Therefore, distributed generation systems can be considered one of the energy supply sources for a more resilient energy system. Indeed, the PV power plant share is expected to increase in RTAS, and nuclear and wind power plants are also expected to play a vital role in the electricity generation mix during this scenario.

Fig. 11 shows the share of solar power plants in the electricity supply over ten-year periods. As can be seen, the PV power plant share is expected to increase from 30% to 65% (in 2060) and from 0% to 36% in RTAS and BAUAS respectively. The large share of solar power plants in Scenario RTAS is the existing policies in Scenario based on the significant share of renewable energy in the power plant portfolio in line with environmental protection policies. In this scenario, it is assumed that

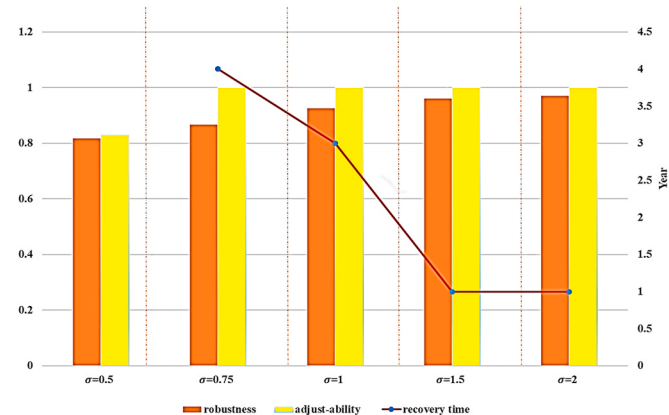


Fig. 13. Vulnerability indicators of the energy system in different σ in BAUAS scenario.

solar energy fluctuations are managed by the synchronicity of energy demand and supply. The noteworthy point in this scenario is the resilience of the energy supply system against the drought disturbance caused by the optimal design of the system and the share of solar energy.

Model results show that the energy system in the RTAS scenario is vulnerable, and the system can adapt itself to change in the climate. The resilience index is equivalent to the cumulative energy needed but not supplied, which according to Table 2, the optimal resilience index in

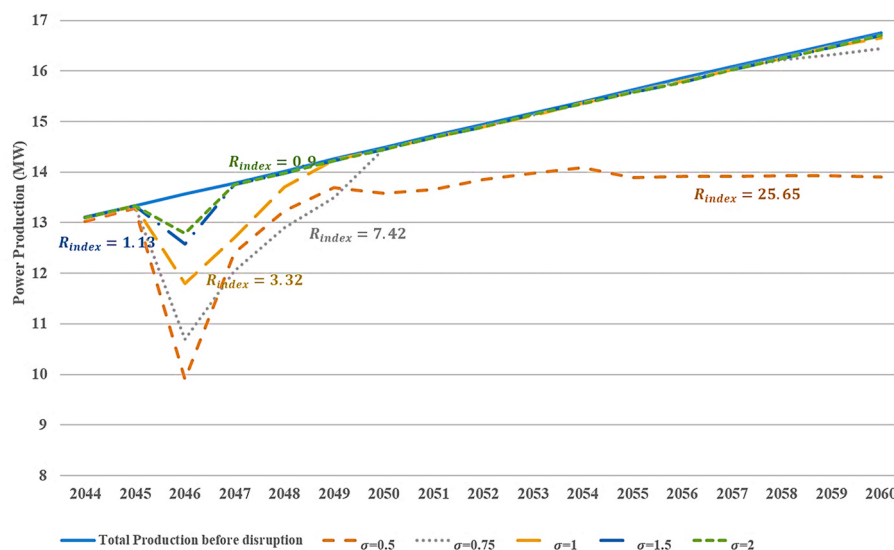


Fig. 12. power production of the system in different σ in BAUAS scenario.

Scenario NAS is 12.76 PJ. Also, the lowest unmet demand in Scenario BAUAS is 3.32, and this index is 0.86 in the optimal state of the system facing disruptive events in Scenario RTAS. Comparison of this index in three scenarios shows that the optimal design of the energy supply system in Scenario RTAS has caused the system performance to be better after the disruption and the energy system is more compatible with the disruption. Therefore, the structure of the system will be very effective in its performance.

The behavior of the energy system is shown by the adjustability index using comparing the optimal performance of the system before and after the disruption occurrence (after the recovery period). If this index is greater than, equal to, or less than one, the behavior of the system is adaptive, robust, or ductile respectively. Examination of this index in Table 2 shows that in all three scenarios, the behavior of the energy supply system is robust. Although the readjustability of the system in the three scenarios are the same, the recovery time of the system in RTAS is one-fifth of it in NAS and one-third of it in BAUAS. Therefore, the rapidity of the energy system for readjusting is higher than the energy system in the RTAS scenario. On the other hand, the system is more robust in the RTAS scenario (see Table 2).

The parameter σ in Equation (21) models the decision-maker's tendency towards more profitable system planning and energy resilient strategies. Large values of σ illustrate a system planner concerned by energy resilience issues at the total cost of the system and vice versa. Indeed, this parameter provides the trade-off between minimizing total cost and mitigating the HILP risk. Figs. 12 and 13 demonstrate the sensitive analysis of energy production in the secondary level of Altalntis RES and vulnerability indicators as a function of these crucial parameters in the BAUAS scenario. As can be seen, increasing σ leads to a smaller ENNS and larger R_{index} because more weight is placed on the HILP event in the objective function. The optimal value of the cumulative energy needed but not supplied (R_{index}) in $\sigma = 0.5$ is 25.65 PJ, while if $\sigma = 2$ this value is 0.9, indicating that the severity of system destruction decreases with increasing policy coefficient.

On the other hand, the energy system robustness increase with rising σ and the recovery time decrease. The notable point is if σ is small (for

example, 0.5), the system could not return to a previous stable state, and the adjustability of this is low; thus, the energy system in this state has a ductile behavior after the disruption. On the other hand, the system robustness is less than 0.9 in $\sigma = 0.5$ and 0.75. This means that the decline in system performance immediately after the disruption is substantial, and the higher the policy coefficient, the optimal system design will be such that the least damage will happen to the energy system. As the policy coefficient increases, the robustness of the system gets closer to one. Also, since the system behavior is ductile in $\sigma = 0.5$, the system performance will not return to its equilibrium state after the disturbance. Nevertheless, if $\sigma = 1.5$ and 2, the system performance will return to equilibrium after one year. Therefore, the policy coefficient is one of the most critical issues that should be considered in planning against climate change.

6. Conclusion

The purpose of this paper is to present a tool for energy decision-makers and planners to obtain the most optimal state of the energy system facing HILP disruptive events. According to the framework developed in this article, the policymaking process is specified in four parts; issue/problem identification, assessment of options/policy formulation, adoption and implementation, and policy evaluation and monitoring. The position of the proposed model in this process is shown in Fig. 14. Identifying current situations of the energy system, reference energy system curve, and HILP events are the main steps to organize the problem. Developing the energy system resilience model, scenarios, and resilience indicators are the main phases of policy formulation. In the adoption and implementation of the policy, the optimal states of the energy system before and after HILP events are calculated in different scenarios, and the policy is evaluated using the calculation of energy resilience indicators and discussing related results.

Indeed, this paper presents a long-term optimization framework to identify the optimum energy system resilience against HILP caused by climate change. The model bridges the gap between long-term energy system planning at a macro level and short-term switching operations or

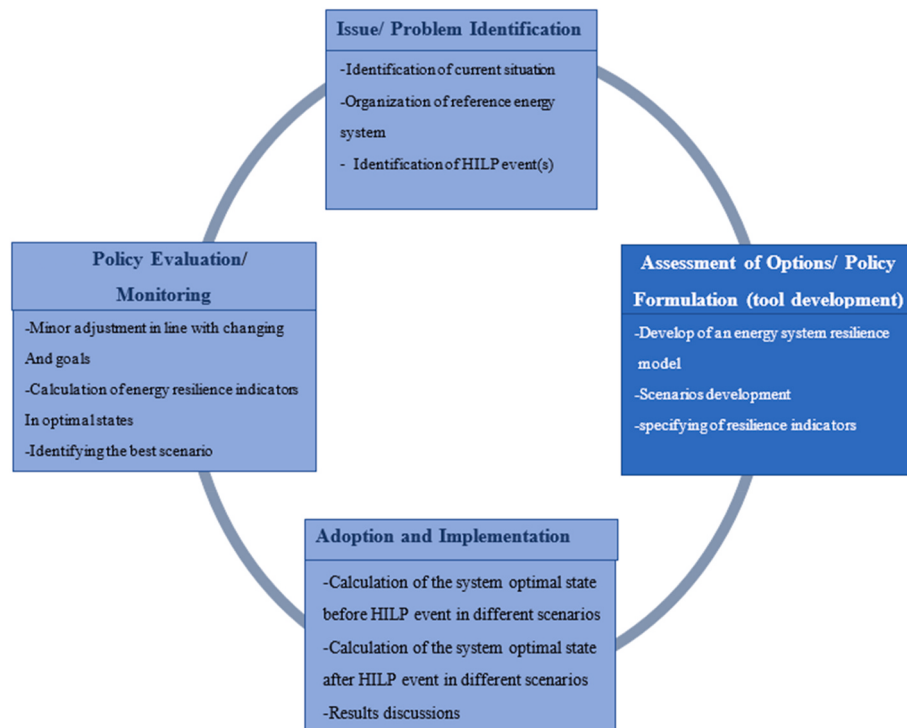


Fig. 14. Policymaking process for energy system resilience.

micro-level modeling approach in response to attacks. The proposed model is structured as a two-stage optimization model to evaluate the resilience for long-term energy planning considering economic, technical, and environmental features, parameter, and constrain sets in the supply system. Also, the structure matrix is designed to identify the interactions between the energy system and the vulnerable points for each HILP event resulting from climate change. The problem is solved by a solution algorithm that allows trade-offs between resilience (ENNS) and economic objectives. Applying this tool offers a high potential for presenting energy planning in an uncertain environment.

The application to a case study shows hydropower is expected to play a vital role in supplying the electricity affected by increasing temperature resulting from climate change. An increase in temperature and extreme temperatures are the main aspects of climate change as a HILP event that affects Atlantis energy system technologies by external costs. We observe that share of electricity generation shifts from coal and hydropower to PV in different scenarios based on the maximization of energy system resiliency. Actually, the faster occurring this shift, the greater vulnerability of the system. Indeed, resilience and robustness of the energy system rise with the switching of PV, and the recovery time of disrupted system decrease to one-fifth in RTAS strategy. Furthermore, the sensitivity analysis of the optimum solution shows that the vulnerability of energy systems against HILP events depends on planner flexibility. There is a trade-off between the total cost of the system in a normal situation and ENNS cost in disruptive situations, and this tool can help decision-makers for allocating an optimal fixed budget to keep the system more resilient.

F_{kjilt}	Consumption of energy in technology type τ for producing useful energy j converting final energy k in sector i at load zone l and time point t
D_{jilt}	Demand for useful energy j in sector i and time point t
η_{kjilt}	The efficiency of end-use appliance that converts energy k into useful energy j in sector i
α_{jil}	Share of load zone l in useful energy demand j in sector i
Δl	Time length of load zone
$Y_{k\tau jilo}$	New build capacity of technology type τ for converting energy carrier k into useful energy j in sector i at time point ω where ω is a point from 1 to t
PF_{kjilt}	Plant factor of technology type τ for converting energy carrier k into useful energy j in sector i at time point t
$H_{kjil\theta}$	Historical capacity of technology type τ for converting energy carrier k into useful energy j in sector i at time point θ , where θ is a point from $(b - \theta)$ to b and b is the base year, and PL is the plant service life.
$T_{k\delta lt}$	The input of energy carrier k to distribution technology δ in load zone l and time point t
$\eta'_{k\delta lt}$	The efficiency of distribution technology δ in load zone l and time point t
$Y_{k\delta kl\omega}$	New build capacity of technology type δ for distributing energy carrier k at time point ω where ω is a point from 1 to t
$PF_{k\delta kl\omega}$	Plant factor of technology type δ for distributing energy carrier k at time point t
$H_{k\delta k\theta}$	Historical capacity of technology type δ for distributing energy carrier k at time point θ , where θ is a point from $(b - \theta)$ to b and b is the base year and PL is the plant service life.
$U_{e\mu kt}$	The input of energy carrier e to conversion technologies μ in load zone l and time point t
$\eta'_{e\mu kt}$	The efficiency of conversion technology μ in load zone l and time point t
$Y_{e\mu k\omega}$	New build capacity of technology type μ for converting energy carrier e at time point ω where ω is a point from 1 to t
$PF_{e\mu k\omega}$	Plant factor of technology type μ for converting energy carrier e at time point t
$H_{e\mu k\theta}$	Historical capacity of technology type μ for converting energy carrier e at time point θ , where θ is a point from $(b - \theta)$ to b and b is the base year and PL is the plant service life.
P_{oyelt}	The input of energy carrier o to processing technology γ in load zone l and time point t
η'''_{oyelt}	The efficiency of processing technology γ in load zone l and time point t
Y_{oyelt}	New build capacity of technology type γ for processing energy carrier o at time point ω where ω is a point from 1 to t
PF_{oyelt}	Plant factor of technology type γ for processing energy carrier o at time point t
H_{oyelt}	

(continued on next column)

(continued)

D_{ot}	Historical capacity of technology type γ for processing energy carrier o at time point θ , where θ is a point from $(b - \theta)$ to b and b is the base year and PL is the plant service life.
T	Additional resources discovered for fossil fuels and resources potential for renewable energies at time t
I_{olt}	Planning time horizon
B_{ot}	Import of energy o in load zone l ant time point t
b_{opt}	Total consumption of resource o in the whole energy supply system at time point t
X_{pt}	Resource use intensity (i.e., consumption of resource o per unit activity of control volume) of type o in control volume ρ at time t
β_{ot}	State variable of control volume ρ (i.e., the activity level of technology ρ) at time point t
P_{at}	The upper limit on the total consumption of resources o in the whole energy supply system at time point t
p_{apt}	The total emission of pollutant a in the whole energy supply system at time point t
ψ_{at}	Emission factor (i.e., emission of pollutant a per-unit activity of control volume) of pollutant a in control volume ρ at time point t
$K_{\varphi tt}$	The upper limit on the total emission of pollutant a in the whole energy supply system at time point t
$Y_{\varphi tt}$	Capital cost per unit capacity of sub-system φ and technology τ at time point t
r_t	The capacity buildup of sub-system φ and technology τ at time point t
\bar{K}	Discount rate at time point t
$m_{\varphi tt}$	Present value of total capital costs of the whole energy supply systems
$c_{\varphi ltt}$	Maintenance costs per unit capacity of sub-system φ and technology τ at time point t
$Y_{\varphi t\omega}$	Capacity builds up of sub-system φ and technology τ at time point ω
$H_{\varphi t\omega}$	The historical capacity of sub-system φ and technology τ at time point t
\bar{M}	Present value of total maintenance costs of the whole energy supply system
$c_{\varphi ltt}$	Operation costs per unit main output of sub-system φ and technology τ in load zone l at time point t
$X_{\varphi ltt}$	Input to technology τ in load zone l at time point t
$\eta_{\varphi tt}$	The efficiency of sub-system φ and technology τ at time point t
\bar{C}	Present value of total operating costs of the whole energy supply system
$v_{\varphi tl}$	Resource costs per sources/import costs per energy carrier φ and load zone l at time point t
$R_{\varphi tl}$	Production of resource/import costs per energy carrier φ and load zone l at time point t
\bar{R}	Present value of total resource costs of the whole energy supply system
e_{klt}	The externality of pollutant k in load zone l and time point t
$\gamma_{\varphi ktl}$	The emission factor of pollutant k in sub-system φ and technology τ in load zone l at time point t
\bar{E}	Present value of total externalities of pollution from the whole energy supply system related to flow
$TPSE_1$	Total primary supply energy resulting from stage 1
$TPSE_2$	Total primary supply energy resulting from stage 2
R_{index}	Resilience index
F_s	The stable system performance level just before the HILP event
F_d	The stable performance level immediately after the HILP event
F_F	The performance level at the new stable level. The recovery reaches its final stage, and the system satisfies the required service.
c_{ji}	The penalty coefficient in useful energy demand j in sector i

Credit author statement

Somayeh Ahmadi: Conceptualization, Methodology, Software, Data curation, Investigation, Formal analysis, Writing – original draft preparation, **Amir Hossein Fakhehi Khorasani:** Conceptualization, Methodology, Formal analysis, Writing – original draft preparation, **Ali Vakili:** Project administration, Conceptualization, Methodology, **Yadollah Saboohi:** Project administration, Conceptualization, Methodology, **Georgios Tsatsaronis:** Conceptualization, Supervision, Writing - Review.

Declaration of competing interest

The authors declare that they have no known competing financial interests or personal relationships that could have appeared to influence the work reported in this paper.

Appendix 1. Verification

The presented energy system as the case study is called “UTOPIA” which was used as a standard example in some models as MARKAL [48] and OSemOSYS [49]. To be compatible with the proposed model, RES of this energy system is drawn like what shown in Fig. A.1. In UTOPIA, there are three energy levels (sources, intermediate and demand) which should supply three useful energy demands: lighting, heating, and transport. The energy needed for heating is provided by electricity and diesel in electrical heater (RHE) and diesel heater (RHO); and the transport energy demand is supplied by electric vehicles (TXE), diesel vehicles (TXD), and gasoline vehicles (TXG). More lighting technology (RL1) requires more lighting at night, and more heating is required in winter. There are two different types of technologies at the intermediate level: energy conversion and processing. Five types of power plants are used for generating electricity in UTOPIA; coal power plant (E01), nuclear power plant (E21), hydropower plant (E31), pumped-storage power plant (E51), and diesel power plant (E70). Diesel and gasoline can be produced by oil refineries (SRE) at an intermediate level and can be imported and placed at the resource level. Fundamental relations and constraints of the proposed model in UTOPIA are presented in Table A1.

Table A.1

Underlying formulation of the proposed model in UTOPIA.

$\begin{aligned} & \forall \tau \in [RL1, RHE, RHO, TXE, TXD, TXG], \\ & \forall j \in [\text{lighting, heating, passenger's Km}], \\ & \sum_{k=1}^m \sum_{t=1}^n F_{kjlt} \times \eta_{kjlt} \geq D_{jlt} \quad \forall j \in [\text{gasoline, diesel, Elec}] \\ & \forall l \in [ID, IN, SD, SN, WD, WN] \\ & \& \forall t \in \text{planning years} \end{aligned}$	A.1
$\begin{aligned} & \frac{F_{kjlt} \times \eta_{kjlt}}{\Delta t} - \sum_{\omega=t-PL}^t Y_{kjil\omega} \times PF_{kjilt} \leq \sum_{\theta=b-(PL-t)}^b H_{kjil\theta} \times PF_{kjilt} \\ & \forall k \in [\text{gasoline, diesel, Elec}] \\ & \forall l \in [ID, IN, SD, SN, WD, WN] \\ & \forall 1 < \omega < t \\ & \& \forall t \in \text{planning years}, b = 2010 \end{aligned}$	A.2
$\begin{aligned} & \sum_{e=1}^{m''} \sum_{\mu=1}^{n''} U_{epklt} \times \eta_{epklt}'' = \sum_{t=1}^n F_{kjlt} \quad \forall e \in [\text{coal, uranium, gasoline, hydro, diesel}] \\ & \& \forall l \in [ID, IN, SD, SN, WD, WN] \\ & \& \forall t \in \text{planning years} \end{aligned}$	A.3
$\begin{aligned} & \frac{U_{epklt} \times \eta_{epklt}''}{\Delta t} - \sum_{\omega=t-PL}^t Y_{epkl\omega} \times PF_{epklt\omega} \leq \sum_{\theta=b-(PL-t)}^b H_{epkl\theta} \times PF_{epklt\theta} \quad \forall l \in [ID, IN, SD, SN, WD, WN] \\ & \forall e \in [\text{coal, uranium, gasoline, hydro, diesel}] \\ & \forall 1 < \omega < t \\ & \& \forall t \in \text{planning years} \end{aligned}$	A.4
$\begin{aligned} & P_{eklt} \times \eta_{eklt}''' = \sum_{t=1}^n F_{kjlt} \quad \forall e = \text{crude oil} \\ & \& \forall l \in [ID, IN, SD, SN, WD, WN] \\ & \& \forall t \in \text{planning years} \end{aligned}$	A.5
$\begin{aligned} & \frac{P_{eklt} \times \eta_{eklt}'''}{\Delta t} - \sum_{\omega=t-PL}^t Y_{ekl\omega} \times PF_{ekl\omega} \leq \sum_{\theta=b-(PL-t)}^b H_{ekl\theta} \times PF_{ekl\theta} \quad \forall l \in [ID, IN, SD, SN, WD, WN] \\ & \forall e = \text{crude oil} \\ & \forall 1 < \omega < t \\ & \& \forall t \in \text{planning years} \end{aligned}$	A.6
$\begin{aligned} & \sum_{t=1}^T \sum_{l=1}^V \sum_{r=1}^{n'''} P_{erlt} \leq \sum_{l=1}^V \sum_{t=1}^T I_{et} \quad \forall e \in [\text{coal, uranium, gasoline, hydro, diesel, crude oil}] \\ & \& \forall l \in [ID, IN, SD, SN, WD, WN] \\ & \& \forall r \in \text{planning years} \end{aligned}$	A.7
$\begin{aligned} & X_{pt} = \lambda_{pt} \quad \forall p \in [E01, E51, RHE, SRE, TXG] \\ & \geq P_{at} = \sum_p p_{apt} \times X_{pt} \leq \psi_{at} \quad \forall a \in \text{pollutants} \& \forall p \in \text{control volumes} \end{aligned}$	A.8
$Z = \min(\bar{K} + \bar{M} + \bar{C} + \bar{R} + \bar{E})$	A.10
$\bar{K} = \sum_{t=1}^T \sum_{\varphi} \sum_{\tau} \left[\frac{k_{\varphi\tau} \times Y_{\varphi\tau t}}{(1+r_t)^t} \right] \quad \forall a \in \text{sub-systems} \& \forall \rho \in \text{planning years} \& \forall \tau \in [RL1, RHE, RHO, TXE, TXD, TXG]$	A.11
$\bar{M} = \sum_{t=1}^T \sum_{\varphi} \sum_{\tau} \left[\frac{m_{\varphi\tau} \times \left(\sum_{o=1}^t Y_{\varphi\tau o} + H_{\varphi\tau t} \right)}{(1+r_t)^t} \right] \quad \forall a \in \text{sub-systems} \& \forall \rho \in \text{planning years} \& \forall \tau \in [RL1, RHE, RHO, TXE, TXD, TXG]$	A.12
$\bar{C} = \sum_{t=1}^T \sum_{\varphi} \sum_{\tau} \sum_l \left[\frac{c_{\varphi\tau lt} \times X_{\varphi\tau lt} \times \eta_{\varphi\tau lt}}{(1+r_t)^t} \right] \quad \forall a \in \text{sub-systems} \& \forall \rho \in \text{planning years} \& \forall \tau \in [E01, E21, E31, E51, E71, SRE]$	A.13
$\bar{R} = \sum_{t=1}^T \sum_{\varphi} \sum_l \left[\frac{v_{\varphi\tau dl} \times R_{\varphi\tau dl}}{(1+r_t)^t} \right] \quad \forall a \in \text{sub-systems} \& \forall \rho \in \text{planning years} \& \forall \tau \in [RL1, RHE, RHO, TXE, TXD, TXG]$	A.14
$\bar{E} = \sum_{t=1}^T \sum_{\varphi} \sum_{\tau} \sum_k \left[\frac{e_{k\tau lt} \times \gamma_{\varphi k\tau lt} \times X_{\varphi\tau lt} \times \eta_{\varphi\tau lt}}{(1+r_t)^t} \right] \quad \forall a \in \text{sub-systems} \& \forall \rho \in \text{planning years} \& \forall \tau \in [E01, E21, E31, E51, E71, SRE]$	A.15

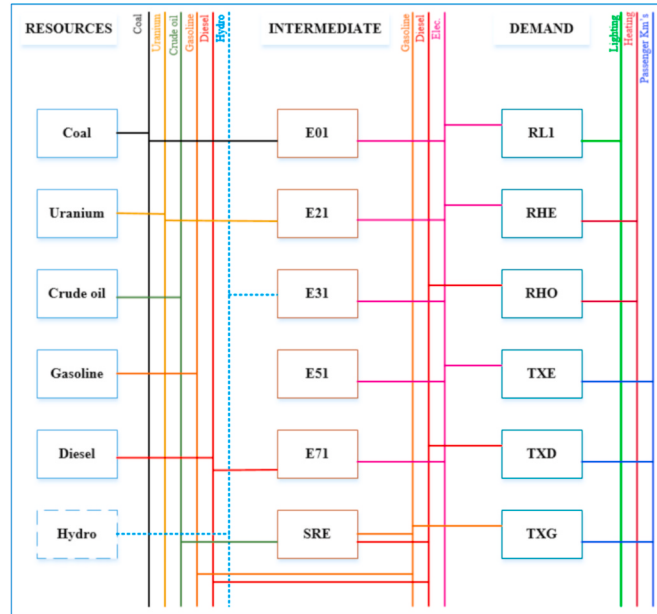


Fig. A.1. The UTOPIA reference energy system (RES).

For verification of proposed model in first stage optimization model, OSeMOSYS source code and data set of UTOPIA were downloaded from Ref. [54], and it was also cited in Table 3 of ref [49] as UTOPIA input data. The results of running UTOPIA by OSeMOSYS and our proposed model in two categories of power generation and end-use capacity are presented in Fig A2.

The objective function value in our proposed model is \$29.2 billion and \$28.8 billion in OSeMOSYS, and both modes are generated almost identical optimization trends for technologies selection so that, as we can see in Fig A2, results are closely reported with power generation and end-use capacity in different technologies.

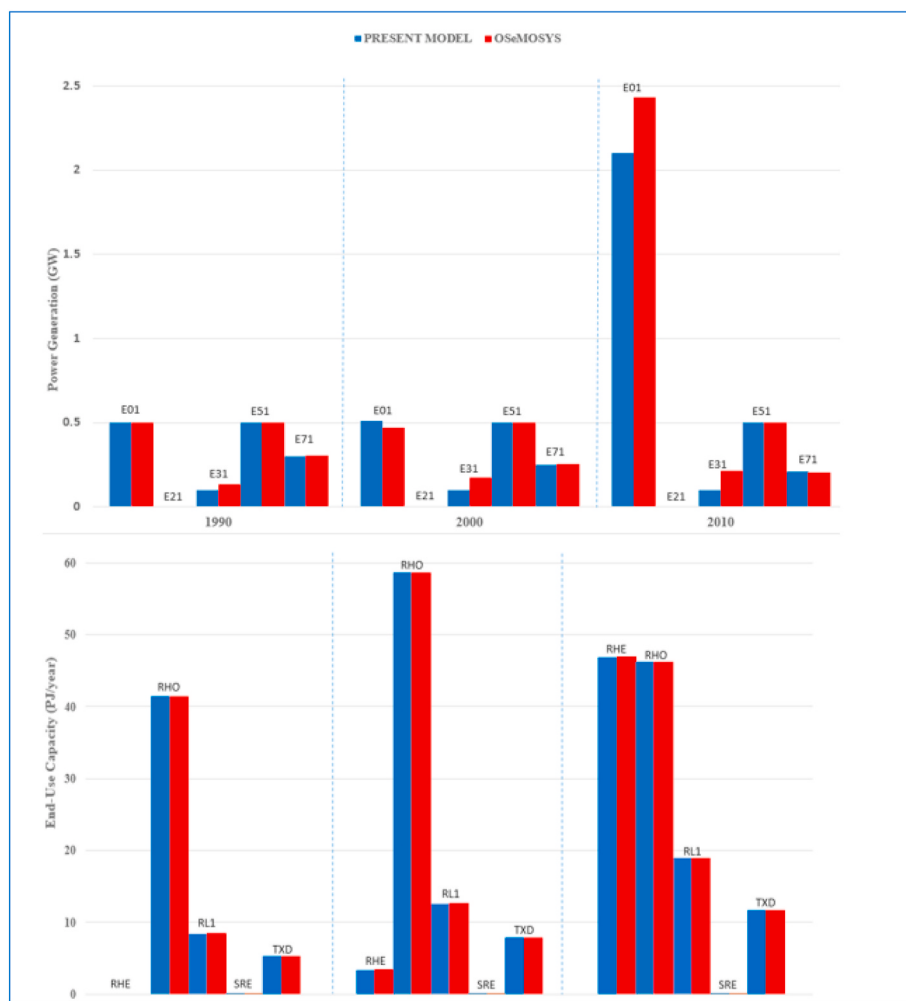


Fig. A.2. Comparison between results of Present model (blue bars) and OSeMOSYS (red bars) for UTOPIA.

References

- [1] S. Moslehi, T.A. Reddy, Sustainability of integrated energy systems: a performance-based resilience assessment methodology, *Appl. Energy* 228 (Oct. 2018) 487–498.
- [2] S. Hosseini, D. Ivanov, A. Dolgui, Review of quantitative methods for supply chain resilience analysis, *Transp. Res. Part E Logist. Transp.* 125 (May 2019) 285–307.
- [3] J. Wang, W. Zuo, L. Rhode-Barbarigos, X. Lu, J. Wang, Y. Lin, Literature review on modeling and simulation of energy infrastructures from a resilience perspective, *Reliab. Eng. Syst. Saf.* 183 (Mar. 2019) 360–373.
- [4] M. Mehri Arsoom, S.M. Moghaddas-Tafreshi, Peer-to-peer energy bartering for the resilience response enhancement of networked microgrids, *Appl. Energy* 261 (Mar. 2020) 114413.
- [5] D. Rehak, P. Senovsky, M. Hromada, T. Lovecek, Complex approach to assessing resilience of critical infrastructure elements, *Int. J. Crit. Infrastruct. Prot.* 25 (Jun. 2019) 125–138.
- [6] L.M. Shakou, J.L. Wybo, G. Reniers, G. Boustras, Developing an innovative framework for enhancing the resilience of critical infrastructure to climate change, *Saf. Sci.* 118 (Oct. 2019) 364–378.
- [7] A.A. Londoño Pineda, O.A. Vélez Rojas (Oscar), M.P. Jonathan, S.B. Sujitha, Evaluation of climate change adaptation in the energy generation sector in Colombia via a composite index — a monitoring tool for government policies and actions, *J. Environ. Manag.* 250 (Nov. 2019) 109453.
- [8] B. Wang, Q. Wang, Y.M. Wei, Z.P. Li, Role of renewable energy in China's energy security and climate change mitigation: an index decomposition analysis, *Renew. Sustain. Energy Rev.* 90 (01-Jul-2018) 187–194. Elsevier Ltd.
- [9] S. Espinoza, M. Panteli, P. Mancarella, H. Rudnick, Multi-phase assessment and adaptation of power systems resilience to natural hazards, *Elec. Power Syst. Res.* 136 (2016) 352–361.
- [10] M. Panteli, D.N. Trakas, P. Mancarella, N.D. Hatziargyriou, Power systems resilience assessment: hardening and smart operational enhancement strategies, *Proc. IEEE* 105 (7) (Jul. 2017) 1202–1213.
- [11] M. Panteli, P. Mancarella, The grid: stronger, bigger, smarter?: presenting a conceptual framework of power system resilience, *IEEE Power Energy Mag.* 13 (3) (May 2015) 58–66.
- [12] Y.-P. Fang, E. Zio, An adaptive robust framework for the optimization of the resilience of interdependent infrastructures under natural hazards, *Eur. J. Oper. Res.* 276 (3) (Aug. 2019) 1119–1136.
- [13] F.H. Jufri, V. Widiputra, J. Jung, State-of-the-art review on power grid resilience to extreme weather events: definitions, frameworks, quantitative assessment methodologies, and enhancement strategies, *Appl. Energy* 239 (January) (2019) 1049–1065.
- [14] Y. Sheffi, J.B. Rice, A supply chain view of the resilient enterprise, *MIT Sloan Manag. Rev.* 47 (1) (Sep-2005).
- [15] Cambridge University Press, *Climate Change 2014 – Impacts, Adaptation and Vulnerability: Regional Aspects - Google Books*, Cambridge University Press, 2014.
- [16] T. Busch, Organizational adaptation to disruptions in the natural environment: the case of climate change, *Scand. J. Manag.* 27 (4) (Dec. 2011) 389–404.
- [17] A.M. Feldpausch-Parker, T.R. Peterson, J.C. Stephens, E.J. Wilson, Smart grid electricity system planning and climate disruptions: a review of climate and energy discourse post-Superstorm Sandy, *Renew. Sustain. Energy Rev.* 82 (01-Feb-2018) 1961–1968. Elsevier Ltd.
- [18] P. Hines, J. Apt, S. Talukdar, Large blackouts in North America: historical trends and policy implications, *Energy Pol.* 37 (12) (Dec. 2009) 5249–5259.
- [19] Y. Almoghathawi, K. Barker, L.A. Albert, Resilience-driven restoration model for interdependent infrastructure networks, *Reliab. Eng. Syst. Saf.* 185 (2019) 12–23.
- [20] N. Nezamoddini, S. Mousavian, M. Erol-Kantarci, A risk optimization model for enhanced power grid resilience against physical attacks, *Elec. Power Syst. Res.* 143 (Feb. 2017) 329–338.
- [21] A. Uemichi, M. Yagi, R. Oikawa, Y. Yamasaki, S. Kaneko, Multi-objective optimization to determine installation capacity of distributed power generation equipment considering energy-resilience against disasters,” in, *Energy Proc.* 158 (2019) 6538–6543.

- [22] S.D. Manshadi, M.E. Khodayar, Resilient operation of multiple energy carrier microgrids, *IEEE Trans. Smart Grid* 6 (5) (2015) 2283–2292.
- [23] A. Arif, Z. Wang, J. Wang, C. Chen, Power distribution system outage management with Co-optimization of repairs, reconfiguration, and DG dispatch, *IEEE Trans. Smart Grid* 9 (5) (Sep. 2018) 4109–4118.
- [24] B. Chen, C. Chen, J. Wang, K.L. Butler-Purry, Sequential service restoration for unbalanced distribution systems and microgrids, *IEEE Trans. Power Syst.* 33 (2) (Mar. 2018) 1507–1520.
- [25] T. Ding, Y. Lin, G. Li, Z. Bie, A new model for resilient distribution systems by microgrids formation, *IEEE Trans. Power Syst.* 32 (5) (Sep. 2017) 4145–4147.
- [26] S.D. Manshadi, M.E. Khodayar, Resilient operation of multiple energy carrier microgrids, *IEEE Trans. Smart Grid* 6 (5) (Sep. 2015) 2283–2292.
- [27] W. Yuan, J. Wang, F. Qiu, C. Chen, C. Kang, B. Zeng, Robust optimization-based resilient distribution network planning against natural disasters, *IEEE Trans. Smart Grid* 7 (6) (Nov. 2016) 2817–2826.
- [28] Y. Fang, G. Sansavini, Optimizing power system investments and resilience against attacks, *Reliab. Eng. Syst. Saf.* 159 (Mar. 2017) 161–173.
- [29] A. Löschel, Technological change in economic models of environmental policy: a survey, *Ecol. Econ.* 43 (2–3) (Dec. 2002) 105–126.
- [30] A. Krook-Rielkola, C. Berg, E.O. Ahlgren, P. Söderholm, Challenges in top-down and bottom-up soft-linking: lessons from linking a Swedish energy system model with a CGE model, *Energy* 141 (Dec. 2017) 803–817.
- [31] A.M. Madni, S. Jackson, Towards a conceptual framework for resilience engineering, *IEEE Syst. J.* 3 (2) (2009) 181–191.
- [32] L. Fraccascia, I. Giannoccaro, V. Albino, Resilience of complex systems: state of the art and directions for future research, *Complexity* 2018 (2018). Hindawi Limited.
- [33] A.M.A. Saja, A. Goonetilleke, M. Teo, A.M. Ziyath, A critical review of social resilience assessment frameworks in disaster management, *Int. J. Disaster Risk Reduc.* 35 (01-Apr-2019). Elsevier Ltd.
- [34] T.E. Grantham, J.H. Matthews, B.P. Bledsoe, Shifting currents: managing freshwater systems for ecological resilience in a changing climate, *Water Secur.* 8 (01-Dec-2019). Elsevier B.V.
- [35] S. Pashapour, A. Bozorgi-Amiri, A. Azadeh, S.F. Ghaderi, A. Keramati, Performance optimization of organizations considering economic resilience factors under uncertainty: a case study of a petrochemical plant, *J. Clean. Prod.* 231 (Sep. 2019) 1526–1541.
- [36] D.J. Provan, D.D. Woods, S.W.A. Dekker, A.J. Rae, Safety II professionals: how resilience engineering can transform safety practice, *Reliab. Eng. Syst. Saf.* 195 (01-Mar-2020). Elsevier Ltd.
- [37] I. Energy Agency, *World Energy Balances 2018*, 2018.
- [38] BP, *BP Energy Outlook 2019*, 2019.
- [39] C.B. Field, et al., *Managing the Risks of Extreme Events and Disasters to Advance Climate Change Adaptation: Special Report of the Intergovernmental Panel on Climate Change*, vol. 9781107025066, Cambridge University Press, 2012.
- [40] J. Ahern, From fail-safe to safe-to-fail: sustainability and resilience in the new urban world, *Lands. Urban Plann.* 100 (4) (Apr. 2011) 341–343.
- [41] D.D. Woods, Four concepts for resilience and the implications for the future of resilience engineering, *Reliab. Eng. Syst. Saf.* 141 (Sep. 2015) 5–9.
- [42] H.H. Willis, K. Loa, *Measuring the Resilience of Energy Distribution Systems*, 2015.
- [43] B. Cassottana, L. Shen, L.C. Tang, Modeling the recovery process: a key dimension of resilience, *Reliab. Eng. Syst. Saf.* (May 2019) 106528.
- [44] C.W. Zobel, L. Khanasa, *Characterizing Multi-Event Disaster Resilience*, 2013.
- [45] S. Ahmadi, Y. Saboohi, A. Vakili, Frameworks, quantitative indicators, characters, and modeling approaches to analysis of energy system resilience: a review, *Renew. Sustain. Energy Rev.* 144 (Jul. 2021) 110988.
- [46] S. Ahmadi, Y. Saboohi, G. Tsatsaronis, A. Vakili, Energy system improvement planning under drought condition based on a two-stage optimization model: the desire for sustainability through the promoting of system's resilience, *Energy Rep.* 7 (2021) 3556–3569.
- [47] S.S.H. Toroghi, V.M. Thomas, A framework for the resilience analysis of electric infrastructure systems including temporary generation systems, *Reliab. Eng. Syst. Saf.* 202 (Oct. 2020) 107013.
- [48] MARKAL demo: Utopia — NESCAUM [Online]. Available: http://www.nescaum.org/topics/ne-markal-model/documents/stakeholder-meeting-documents/markal_demo-utopia.ppt/view. (Accessed 30 March 2020).
- [49] M. Howells, et al., OSeMOSYS: the open source energy modeling system. An introduction to its ethos, structure and development, *Energy Pol.* 39 (10) (Oct. 2011) 5850–5870.
- [50] A. Palombelli, F. Gardumi, M.V. Rocco, M. Howells, E. Colombo, Development of functionalities for improved storage modelling in OSeMOSYS, *Energy* 195 (Mar. 2020) 117025.
- [51] GitHub - OSeMOSYS/OSeMOSYS: OSeMOSYS - the open source energy modelling system [Online]. Available: <https://github.com/osemosys/osemosys>. (Accessed 29 August 2020).
- [52] D. Iribarren, M. Martín-Gamboa, Z. Navas-Anguita, D. García-Gusano, J. Dufour, Influence of climate change externalities on the sustainability-oriented prioritisation of prospective energy scenarios, *Energy* 196 (Apr. 2020) 117179.
- [53] D. Raje, P. Mujumdar, Reservoir performance under uncertainty in hydrologic impacts of climate change, *Adv. Water Resour.* 33 (3) (Mar. 2010) 312–326. P.
- [54] NTR1 [Online]. Available: <http://www.osemosysmain.yolasite.com/>. (Accessed 14 August 2020).